



ELSEVIER

Available online at www.sciencedirect.com

SCIENCE @ DIRECT®

C. R. Physique 4 (2003) 221–230



Hydrodynamics and physics of soft objects/Hydrodynamique et physique des objets mous

Structure and flow of polyelectrolyte microgels: from suspensions to glasses

Structure et écoulement de microgels polyélectrolytes : de la suspension au verre

Michel Cloitre ^{*}, Régis Borrega ¹, Fabrice Monti, Ludwik Leibler

Laboratoire matière molle et chimie (UMR 167, CNRS/ESPCI/ATOFINA), ESPCI, 10, rue Vauquelin, 75231 Paris cedex, France

Presented by Guy Laval

Abstract

Polyelectrolyte microgels are soft particles due to their ability to de-swell osmotically. In dilute suspensions, they behave like soft Brownian particles. Above close-packing, they form pastes which share many features with glasses. The flow properties of suspensions and pastes are universal. They can be tuned at will to get the rheological behaviour which is desired. *To cite this article: M. Cloitre et al., C. R. Physique 4 (2003).*

© 2003 Académie des sciences/Éditions scientifiques et médicales Elsevier SAS. All rights reserved.

Résumé

Les microgels polyélectrolytes sont des particules colloïdales « molles ». Leur élasticité est dominée par l'entropie de translation des contre-ions. Dans les suspensions diluées, les microgels se comportent comme des particules browniennes susceptibles de se gonfler et de se dégonfler par effet osmotique. A partir d'une concentration en polymère généralement faible, les microgels forment des pâtes dont la dynamique présentent des analogies fortes avec celle des verres. Les propriétés d'écoulement des suspensions et des pâtes sont universelles. Elles peuvent être ajustées à volonté afin d'obtenir le comportement rhéologique recherché. *Pour citer cet article : M. Cloitre et al., C. R. Physique 4 (2003).*

© 2003 Académie des sciences/Éditions scientifiques et médicales Elsevier SAS. Tous droits réservés.

Keywords: Polyelectrolyte microgels; Brownian particles; Pastes

Mots-clés : Microgels polyélectrolytes ; Particules browniennes ; Pâtes

1. Introduction

Colloidal suspensions and polymer systems represent two distinct classes of materials with very different flow properties. In semi-dilute polymer solutions and melts, interactions between monomers are generally short-ranged and the dynamics are controlled by the existence of topological constraints that hinder transverse diffusion of the chains. These systems are viscoelastic. In colloidal suspensions, the dynamics are governed by long-ranged colloidal and hydrodynamic interactions. Dilute suspensions are viscous. They form gels or colloidal glasses and become solids at high concentration. Besides these two extreme

* Corresponding author.

E-mail address: michel.cloitre@espci.fr (M. Cloitre).

¹ Present address: Spontex, Recherche et Développement, 74, rue de Saint-Just-des-Marais, 60026 Beauvais cedex, France.

classes of systems, it is now possible to synthesise materials that share common features with polymers and colloids. Classical examples are multi-arm star polymers [1], colloidal particles covered by grafted or adsorbed polymer chains [2], and block copolymer micelles [3]. In these systems, the elementary objects are inherently soft and deformable because of their polymeric nature and at the same time they are partially impenetrable just like colloidal particles. This combination between colloid-like and polymer-like properties opens new routes to design materials with unique properties.

Microgels constitute a particular class of soft materials made of cross-linked latex particles that can be swollen in a solvent [4]. The swelling is generally triggered by chemical or physical stimuli such as temperature, pH or a change of the solvent quality. Microgels have attracted much interest in the past years mainly because of their practical importance in applications [4,5]. Concentrated dispersions are widely used to impart yielding properties to resins in surface coatings and in the printing industries. Alternatively, microgels may be of potential to micro-encapsulate and deliver active molecules in the pharmaceutical industry. In all these applications, it is crucial to understand the relation between the local structure of the individual particles and the dynamical properties of the dispersions.

In the present paper, we consider dispersions of polyelectrolyte microgels consisting of cross-linked copolymer chains bearing ionisable groups which are swollen by water. In polyelectrolyte microgels, it is the osmotic pressure associated with the high translational entropy of the small ions, which is at the origin of the softness of the individual particles. We show that this softness controls most of the flow properties of microgel dispersions and that it is possible to get a desired macroscopic behaviour by tuning the microscopic structure of the individual particles.

Firstly, we analyse how polyelectrolyte microgels swell and how the counter-ions are distributed in the dispersion. In contrast with polyelectrolyte gels, we find that the ion distribution in microgel dispersions results from a subtle exchange between the particles and the surrounding water. The ion distribution is closely coupled with the size and the structure of the individual particles and with the concentration. Therefore the polymer network swells or shrinks depending on the physico-chemical environment and the volume fraction occupied by the particles. At low volume fractions, microgel dispersions behave like hard-sphere suspensions. At high volume fraction, the dynamics are frozen and the dispersions undergo the analogue of a glass transition. Since the individual particles are soft and deformable, it is possible to further increase the volume fraction to get a paste. In pastes, steric constraints between particles are so high that macroscopic flow is not possible unless a finite stress is applied. Below the so-called yield stress, pastes are intrinsically out-of-equilibrium. They exhibit time-dependent phenomena, which can be understood in terms of ageing and rejuvenation, just like in glassy systems. Above the yield stress, pastes flow like viscous suspensions. Surprisingly, although the flow properties appear to be very sensitive to many experimental parameters, they can be described in a universal way.

2. Polyelectrolyte microgels

2.1. Synthesis of microgels

Different methods have been reported for the synthesis of microgel particles [4]. In this work, we prepare polyelectrolyte microgels by standard emulsion polymerisation techniques using the two monomers ethyl acrylate and neutral methacrylic acid, and a di-functional monomer which acts as a cross-linker [6]. It is convenient to characterise the cross-link density by the average number of monomers between two cross-links, N_X . N_X can be easily calculated assuming that one cross-link connects two chain segments and that the different monomers are homogeneously distributed inside the microgels. In the following, we have used three batches of microgels with different amounts of cross-linker ($N_X = 140, 70$ and 28 respectively). The product of a synthesis is a suspension of colloidal particles that are insoluble in water at low pH.

After preparation, suspensions are neutralised with sodium hydroxide solutions. The degree of ionisation can be characterised by the degree of neutralisation, α , which is the molar ratio of the added base to the acid groups available. Upon neutralisation, the acid units become negatively charged causing the swelling of the microgels. Dynamic light scattering at low concentration in the absence of interactions allows us to determine the shape and the characteristic size of the individual particles. Microgels are Brownian spherical particles (Fig. 1). In the collapsed state, the hydrodynamic radius is $R_0 = 50$ nm and the polymer concentration inside the particles is $c_0 \simeq 6$ mole/l. In the swollen state, the hydrodynamic radius R is much larger than R_0 . It is convenient to characterise the swelling of microgels by the swelling ratio $Q = (R/R_0)^3$. The swelling ratio is very sensitive to many experimental parameters such as the conditions of synthesis, the ionic strength of the solution and the cross-link density. Predicting and controlling the swelling behaviour of microgels is an important issue in many applications.

2.2. Swelling and elasticity of polyelectrolyte microgels

Table 1 shows that the volume of the microgels can increase by two orders of magnitude when they swell. Interestingly, this is much larger than the swelling generally measured for microgels in organic solvents [7,8]. This unique property comes from

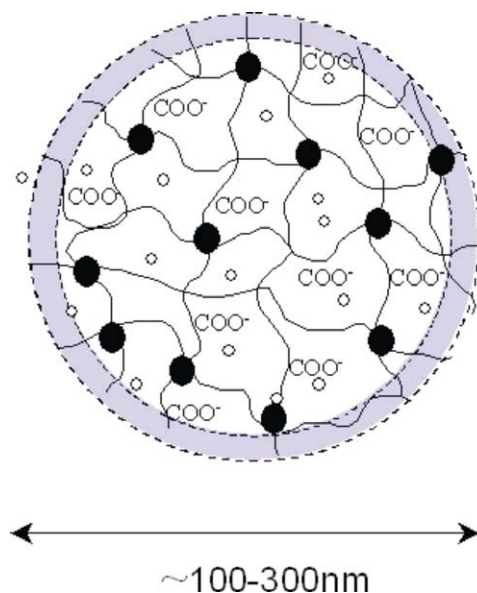


Fig. 1. Schematic representation of a microgel particle in the swollen state. The full dots between chain segments represent the cross-links. Open dots represent the counter-ions. The outer shell represents the region where electro-neutrality is not satisfied locally.

Table 1
The experimental parameters

N_X	R ($\alpha = 1$) (nm)	Q_m ($\alpha = 1$)	K ($\Gamma \cong 0$) (Pa)	C_m (wt%)	Γ (calc/meas)
140	220	85	57000	0.85	0.04/0.10
70	172	39	125000	1.6	0.037/0.08
28	125	16	300000	3.6	0.03/0.06

electrostatic effects: the high translational entropy of the counter-ions associated with the electric charges borne by the network gives rise to strong osmotic effects which dominate the behaviour of polyelectrolyte microgels. In this context, it is tempting to extend to microgels the concepts developed for macroscopic polyelectrolyte gels.

The swelling of polyelectrolyte gels mainly results from the combined action of three contributions [9]: the mixing entropy of the polymer, the osmotic pressure exerted by the counter-ions trapped in the network against the ions in the solution, and the configurational elasticity of the network. In general, the exact solution depends on the quality of the solvent, the ionisation degree, the cross-link density and the ionic strength. In the present work, water is a poor solvent of the polymer. In this case, the microgels are expected to undergo a discontinuous volume-phase transition when the ionisation degree is increased [6,9,10]. When the degree of ionisation is high, the mixing entropy of the polymer can be neglected and the equation of swelling reduces to the balance between the osmotic pressure inside the microgels and the osmotic pressure outside:

$$\Pi_{in} + \Pi_{el} = \Pi_{out}. \quad (1)$$

Π_{in} and Π_{out} are respectively the osmotic pressures of the mobile ions inside the microgels and in the solution. The modulus of the microgels, K , is of the order of the osmotic pressure $\Pi_{in} - \Pi_{out}$. Π_{el} is the elastic pressure of the polymeric network. The terms Π_{in} and Π_{out} can be expressed as:

$$\Pi_{in(out)} = RT C_{in(out)}, \quad (2)$$

where C_{in} and C_{out} are the concentrations of ions inside and outside the microgels. Let us assume that there is no added salt and that all the counter-ions associated with the ionised units are trapped inside the polymeric network by the electrostatic attraction exerted by the fixed charges. Then, C_{out} is 0 and C_{in} is simply the concentration of ionised units inside the microgels: $C_{in} = \alpha c_0 z / Q$ where z is the molar fraction of acidic units. We take for the elastic pressure Π_{el} that of a polymeric network, which is stretched from the collapsed state, taken as the reference state, to the swollen state [9,11]:

$$\Pi_{el} = -\frac{RT c_0}{2N_X Q^{1/3}}. \quad (3)$$

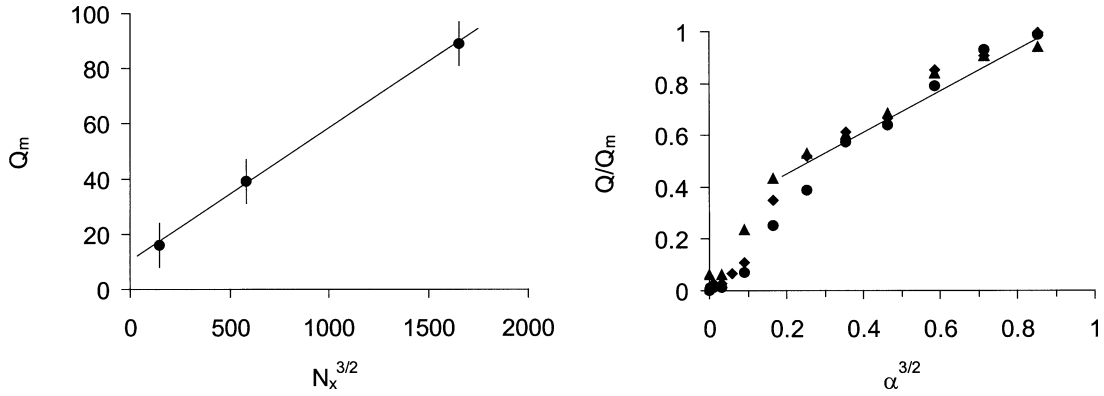


Fig. 2. Left: variation of the swelling ratio at maximum swelling versus the cross-link density. Right: variation of the swelling ratio with the neutralisation degree for $N_X = 140$ (\bullet), $N_X = 70$ (\blacklozenge), $N_X = 28$ (\blacktriangle).

Using relations (1)–(3), we obtain easily the swelling ratio Q of microgels as a function of the ionisation degree and of the cross-link density:

$$Q \propto (\alpha N_X)^{3/2}. \quad (4)$$

In Fig. 2, we compare this prediction with the results of the experimental study. We observe that the swelling ratio at maximum swelling, Q_m , is well proportional to $N_X^{3/2}$ (Fig. 2(a)). It is also interesting to plot the variations of the normalised swelling ratio Q/Q_m as a function of $\alpha^{3/2}$ (Fig. 2(b)). When the ionisation degree is low, Q/Q_m is very small, indicating that the microgels do not swell. As the ionisation degree increases, the swelling ratio rises sharply. We think that this is the signature of a discontinuous volume transition. Above the volume transition, the data measured for the different cross-link densities fall on a single line in nice agreement with the theoretical prediction. In conclusion, at infinite dilution, polyelectrolyte microgels swell like macroscopic gels.

2.3. Osmotic de-swelling

The previous analysis is based on the assumption that all the counter-ions are trapped inside the microgels. To test this hypothesis, we compare the Debye length associated with the counter-ions at concentration C_{in} with the characteristic size of the microgels: $\kappa_{in}^{-1} = (4\pi\ell_B N_A C_{in})^{-1/2}$, where ℓ_B is the Bjerrum length and N_A the Avogadro number. For all the samples investigated, the screening length κ_{in}^{-1} is much smaller than the radius of the particles ($\kappa_{in} R > 50$). Therefore, microgels are almost electro-neutral as a whole. Only, the counter-ions in a peripheral shell of thickness κ_{in}^{-1} can leave the microgels and diffuse in the solution (Fig. 1). The fraction of those counter-ions is: $\Gamma \cong 3\kappa_{in}^{-1}/R$. The corresponding uncompensated charge density borne by a microgel is $Z \cong N_A c_0 z \kappa_{in}^{-1}/Q$. The variation of Γ with the swelling ratio ($\Gamma \sim Q^{1/6}$) is sufficiently slow to consider that it remains equal to its value at infinite dilution. In Table 1, we have reported the values of Γ calculated from the Debye length and the values measured from conductivity experiments. Clearly, a small fraction of counter-ions is not trapped and can diffuse freely in the solution. At a high concentration, the concentration of free counter-ions in the solution can be large enough to induce an osmotic de-swelling of the microgels. A rigorous analysis of the problem requires to calculate self-consistently the swelling and the counter-ion distribution [12]. However, the importance of osmotic de-swelling can be quantified using the simple approach which follows.

We still use Eqs. (1), (2) and (3) where C_{in} and C_{out} now take into account the existence of free counter-ions. The new expressions for C_{in} and C_{out} are [11]:

$$C_{in} = \frac{\alpha(1-\Gamma)zc_0}{\tilde{Q}} \quad \text{and} \quad C_{out} = \frac{\alpha\Gamma zc_0}{\tilde{Q}} \frac{\Phi}{1-\Phi}, \quad (5)$$

where \tilde{Q} is the swelling at finite concentration, and Φ is the volume fraction of microgels in the solution. To estimate the effect of osmotic de-swelling, we solve Eq. (1) taking into account (2), (3) and (5). We get the following expression for the swelling ratio at finite concentration, \tilde{Q} , as a function of the swelling ratio at infinite dilution Q :

$$\frac{\tilde{Q}}{Q} = \left[1 - \frac{\Gamma}{1-\Phi} \right]^{3/2}. \quad (6)$$

Using the values of Γ given in Table 1, it is easy to see that the volume of the microgels can be reduced by one third near close packing ($\Phi = 0.6$). The osmotic de-swelling of microgels has important consequences for the flow behaviour of microgels suspensions at high concentration.

3. From colloidal suspensions to concentrated pastes

3.1. Viscosity of dilute suspensions

At low concentration, microgels solutions are purely viscous. The viscosity is constant at low shear-rates and shear thinning at high shear-rates. Fig. 3 depicts typical variations of the low-shear viscosity η_0 with the concentration C . η_0 first increases slowly with the concentration, then rises sharply at a concentration C_m above which it is no longer accessible. In practice, C_m increases with the cross-link density (Table 1). By comparison, the viscosity of uncrosslinked polyelectrolyte chains with the same composition increases smoothly and never diverges. A divergence of the viscosity is one of the characteristic features of the dynamics of colloids. It shows that microgels solutions behave like colloidal suspensions of Brownian particles.

It is interesting to determine the variations of the viscosity η_0 in function of the volume fraction of the microgels Φ . C and Φ are related through the simple relation:

$$\Phi = \frac{\tilde{Q}}{V_m c_0} \frac{\rho_s}{\rho_p} C. \tag{7}$$

V_m is the molar volume of monomeric units. ρ_s and ρ_p are the specific mass of the suspension taken equal to that of water and the specific mass of the polymer ($\rho_p = 1.24 \pm 0.01 \text{ g/cm}^3$). Using the values calculated in the previous section for the swelling ratio, we can easily compute the volume fraction of microgels. In Fig. 4, we have plotted the variations of the relative viscosity η_0/η_s with Φ for the three types of microgels investigated (η_s is the viscosity of the solvent). Within the experimental accuracy, the data collapse nicely on a single curve which is very close to the analytical form expected for polydisperse hard spheres [13]: $\eta_0/\eta_s = (1 - \Phi/\Phi_m)^{-2}$ where $\Phi_m = 0.64$ is the volume fraction at which the viscosity diverges. This result deserves several comments. Firstly, we emphasise that it is crucial to use the swelling ratio at finite concentration, \tilde{Q} , to calculate the volume fraction of microgels. Using the swelling ratio at infinite dilution would lead one to overestimate the volume fraction by a large factor making the divergence of the viscosity smoother. Secondly, the fact that microgel suspensions behave like hard-sphere suspensions indicate that electrostatic effects do not bring any significant contribution to the potential of interaction. This is because the net charge borne by the microgels is small ($Z \cong 0.01 \text{ e/nm}^2$) and because the ionic strength outside the microgels is large.

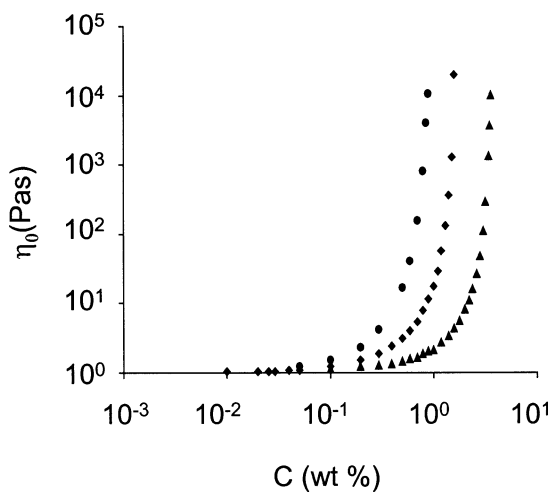


Fig. 3. Variations of the low-shear viscosity of microgel suspensions with the polymer concentration for $N_X = 140$ (●), $N_X = 70$ (◆) and $N_X = 28$ (▲).

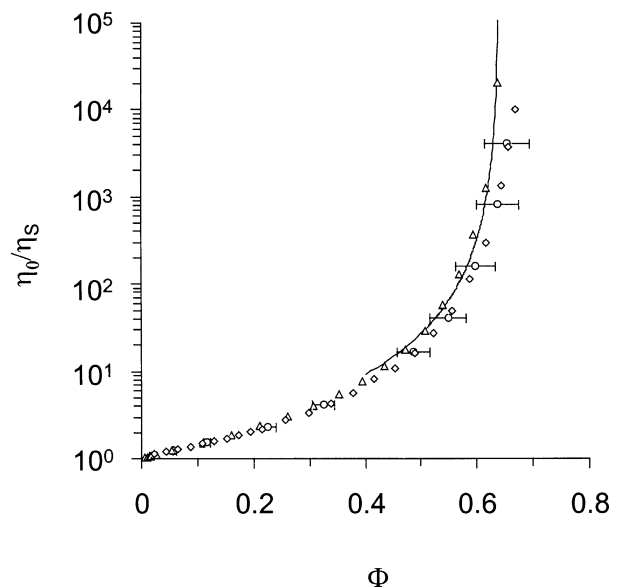


Fig. 4. Variations of the low-shear viscosity with the volume fraction of microgels (○: $N_X = 140$; ◇: $N_X = 70$; △: $N_X = 28$). The full line represents the variation expected for polydisperse brownian hard-spheres.

3.2. Glass-like dynamics of pastes

In contrast to hard colloids, it is possible to concentrate microgel suspensions well above C_m and to get pastes. In this regime of concentration, the swelling of the microgels is governed by osmotic effects and by steric constraints. Since the size and the shape of the microgels are continuously changing, it is not possible to define the volume fraction of the microgels. Therefore, we shall characterise the pastes by the weight concentration C (equivalent to the monomer concentration).

Above C_m , pastes show a solid-like behaviour. Diffusive Wave Spectroscopy allows the efficient non-invasive determination of the structure and of the local dynamics over a wide range of time-scales [14]. In a typical experiment, pastes are seeded with small Polystyrene beads, which strongly scatter light without altering the rheological properties. The pastes are kept at rest during at least 48 hours before any measurement to ensure that the local stresses created during the cell loading have relaxed. The samples are illuminated uniformly by a 1 cm diameter laser beam. Photons undergo a large number of scattering events as they go through the paste. They interfere and form a speckle pattern at the surface of the detector. The time-averaged correlation function of the intensity detected in a speckle varies from point to point: pastes are non-ergodic. Ensemble-averaged intensity correlation functions (ICF) are obtained after averaging the time-averaged correlation functions over a large ensemble of speckles. The ensemble-averaged ICF give access to the mean-square displacements (MSD) of the tracers inside the paste. A typical result is plotted in Fig. 5. It is interesting to note that we follow the motion of the tracers over a wide range of time scales ranging from Brownian time scales to macroscopic time scales.

At long time scales, the MSD exhibits a plateau, which expresses the arrest of the dynamics. This plateau is due to a cage effect: particles cannot move freely through the paste because they are trapped in the cages formed by their neighbours. Particles are trapped over very long times and there is no evidence for long-time relaxation even at the longest time scales investigated. At short time scales, the particles move in their cage. This behaviour is similar to that of a colloidal glass far above the glass transition. In the case of microgels pastes, the MSD is well represented by a stretched exponential: $\langle \Delta r^2(t) \rangle = \delta^2 \{1 - \exp[-(t/\tau_\beta)^\beta]\}$. The exponent β characterises the short time dynamics. The displacement at the plateau δ represents the maximum excursion of the probe particles before their neighbours trap them. The parameter τ_β is the time scale associated with local relaxation.

3.3. Elasticity of pastes

At rest, pastes behave like elastic solids. The elastic modulus can be determined from the particle mobility in the DWS experiment. Indeed, at the maximum excursion, the energy associated with the elastic forces which push back the particles inside their cage must be of the order of kT : $G_0 \delta^2 R = kT$. The values of the elastic modulus that are determined by this method agree with those measured using conventional rheological techniques. In Fig. 6, we show the variations of the elastic modulus G_0 with the relative concentration C/C_m for different microgels. All the curves exhibit the same shape independently

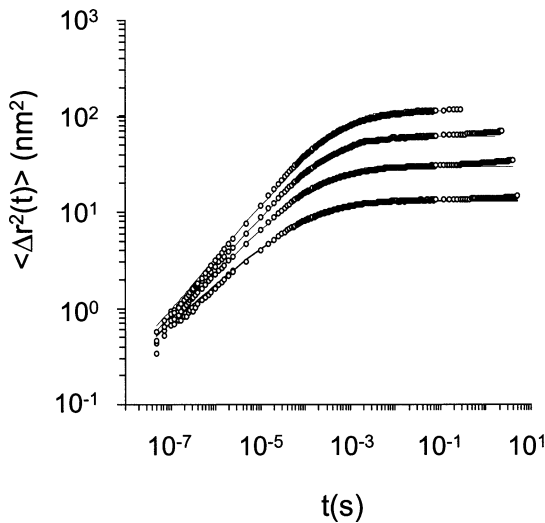


Fig. 5. Mobility of tracers in microgels pastes. From bottom to top: $C = 3$ wt%; $C = 2$ wt%; $C = 1.8$ wt%; $C = 1.6$ wt% ($N_X = 140$). The full lines represent the best fits by stretched-exponentials.

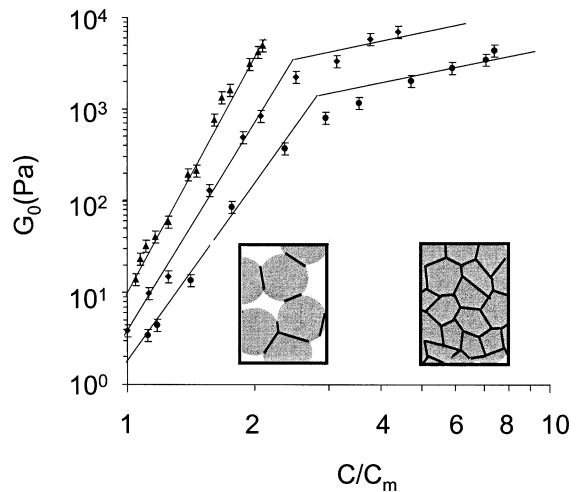


Fig. 6. Variations of the elastic modulus with the concentration for different cross-link densities (\bullet : $N_X = 140$, \blacklozenge : $N_X = 70$, \blacktriangle : $N_X = 28$). The insets show the structure of the pastes below $\Phi = 1$ ($C/C_m < 2$) and for $\Phi = 1$ ($C/C_m > 2$).

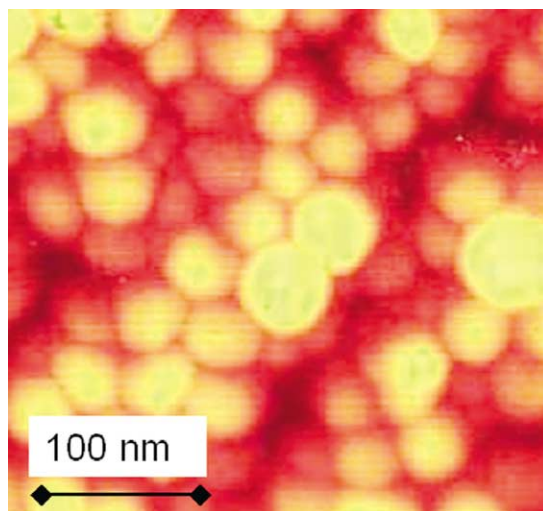


Fig. 7. AFM image of a paste showing the deformation of the individual particles.

of the cross-link density. The elastic modulus first increases as a power law with a large exponent. Above $C/C_m \cong 2$, the increase becomes slower. This regime is not reached in the case of the microgels with the highest cross-linked density because it is not possible to prepare homogeneous pastes at such high concentrations.

To understand these results, it is useful to come back to the local structure. In pastes, packing constraints force the microgels to adapt their volume and their shape by developing flat facets at contact (Fig. 7). Because the number and the size of the facets increase with increasing concentration, microgels progressively take the shape of rounded polyhedrons. These facets can be seen as Hertzian contacts through which microgels exert repulsive forces one on the other. The repulsive force between two elastic spheres depends on the elastic modulus K of the spheres and on the degree of compression [15]. In pastes, the situation is much more complicated because each microgel interacts with many neighbours. Accordingly, the number and the orientation of the facets depend on the concentration and may vary from one particle to another depending on the local neighbourhood. This problem exhibits strong analogies with that of emulsions except that in the latter case, the elasticity results from the deformation of the droplets rather than from their internal elasticity [16,17]. An additional complication comes from the fact that the osmotic modulus of the microgels changes with the concentration because of de-swelling. A rigorous modelling of paste elasticity is beyond the scope of this paper. However, the simple picture of compressed spheres suffices to understand qualitatively the variations of the elastic modulus shown in Fig. 6.

First, we note that the elastic modulus of a paste near C_m is well proportional to the osmotic modulus K of the individual microgels (Table 1). The initial increase of the paste elasticity above C_m is due to the fact that the number of elastically-active microgels increases quickly and that they develop more and more facets in contact. When the volume fraction of microgels becomes equal to 1, the local connectivity does not change any longer but microgels continue to de-swell. In this regime, the variations of the elasticity of the pastes are slower and reflect simply the increase of the osmotic modulus of the individual particles.

4. Paste rheology

4.1. Yielding behaviour

In pastes, steric constraints between particles are so important that the motion of individual particles is drastically reduced. Therefore, we expect that a finite stress is required to make pastes yield and flow. Creep measurements are well adapted to investigate the so-called yielding properties of pastes. In a creep experiment, the paste is loaded in the flow cell of a stress-controlled rheometer, a constant stress is applied at $t = 0$ and the resultant shear-rate response is recorded as a function of time. Typical results are shown in Fig. 8. We find that there exists a particular value of the stress below which the shear-rate never reaches a steady-state value even after very long periods of time. In this regime, pastes behave like plastic solids which creep very slowly without reaching equilibrium. At a slightly higher stress, the shear-rate reaches a steady-state value after a long period of time. The time required to reach steady state becomes shorter for larger stresses. In this regime, pastes behave like viscous liquids. Experimentally, we have defined the yield stress as the lowest value of the shear stress below which steady state is not reached within the typical duration of an experiment.

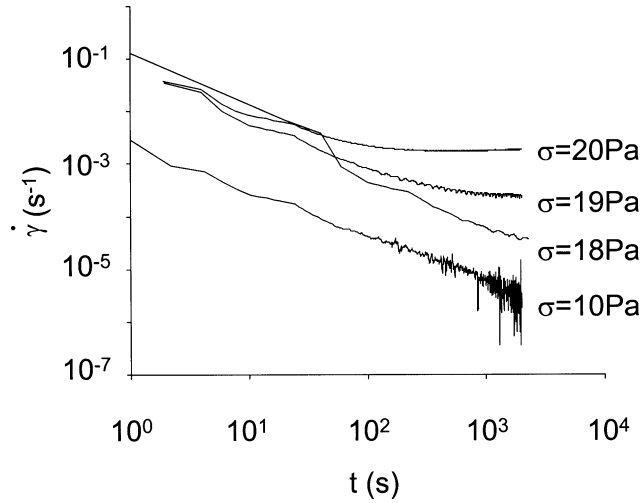


Fig. 8. Time variations of the shear-rate in creep experiments ($N_X = 140$, $C = 2$ wt%). The yield stress is $\sigma_y = 19$ Pa.

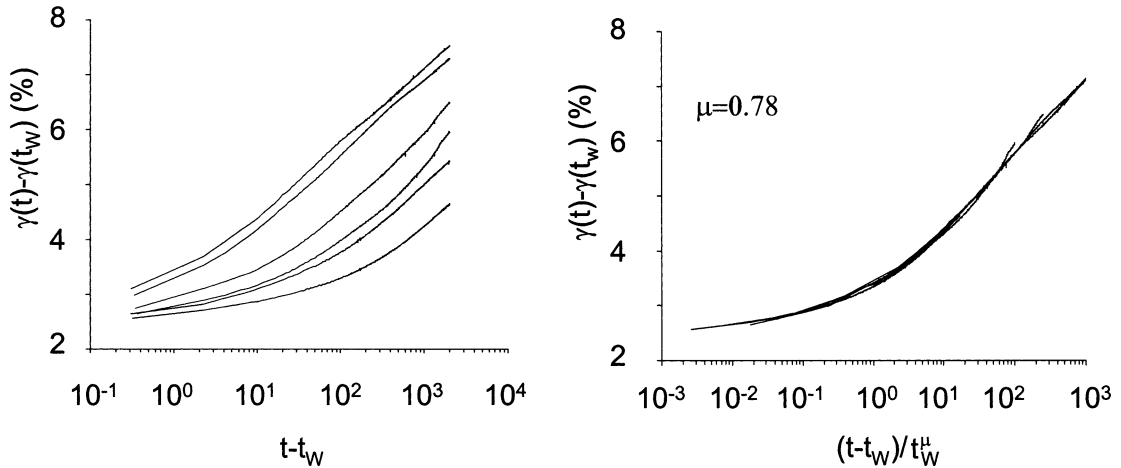


Fig. 9. Left: creep curves measured at different waiting times: $t_W = 15$ s, $t_W = 30$ s, $t_W = 300$ s, $t_W = 1000$ s, $t_W = 2000$ s, and $t_W = 10000$ s (from top to bottom). The amplitude of the stress is $\sigma_m = 10$ Pa. Right: same curves plotted as a function of the ageing variable $(t - t_W) / t_W^{\mu}$.

This protocol can be used to measure the yield stress of microgel pastes when the concentration and the cross-link density are varied. We find that the yield stress is proportional to the linear elastic modulus through a coefficient which represents the yield strain γ_y . This result shows that pastes behave like weak elastic solids up to the yield point and that the yield stress is simply the elastic stress necessary for to escape out of its cage. The yield strain is practically independent of the cross-link density and of the concentration: $\gamma_y = 0.05$. This value is comparable to the yield strain of other soft solids like foams or emulsions [18].

4.2. Slow dynamics and ageing

Below the yield stress, pastes are intrinsically out of equilibrium. A consequence is that measurements are not reproducible unless the initial preparation and the mechanical history are perfectly controlled. Accordingly, we used the following experimental protocol. First, we pre-shear the paste by applying a stress σ_p larger than the yield stress σ_y during a short time interval t_p . This step is designed to erase all internal stresses coming from the loading of the rheometer and to prepare the pastes in a reproducible state. At $t = 0$, the stress is set to zero and the pastes are allowed to rest under zero stress for a time t_W . The rheological properties evolve slowly during this step. At $t = t_W$, we apply a stress σ_m . The time variations of the strain response depend on the amplitude of the stress σ_m . Here we consider the case where σ_m induces plastic flow inside the paste. Fig. 9 shows that the response depends on the waiting time t_W . The initial response at $t = t_W$ is that of an elastic material. The

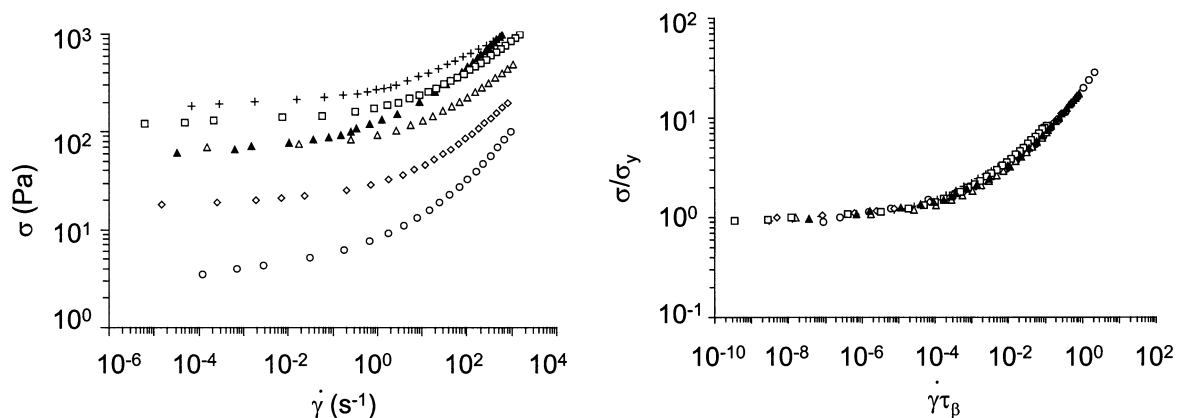


Fig. 10. Left: flow curves for $N_X = 140$. Open symbols: $\eta_S = 1$ mPa·s; $C = 1.5$ wt% (\circ), $C = 2$ wt% (\diamond), $C = 3$ wt% (\triangle), $C = 4$ wt% (\square), $C = 6$ wt% ($+$). Full symbols: $\eta_S = 10$ mPa·s, $C = 3$ wt% (\blacktriangle). Right: same curves plotted in the set of coordinates $(\dot{\gamma}\tau_\beta, \sigma/\sigma_y)$.

response is largest for the smallest waiting times, expressing the fact that the elastic modulus increases with time. Plastic creep follows the initial elastic response. It begins later and is slower for longer waiting times.

To account for the unusual dependence of the mechanical behaviour on the waiting time, it is interesting to introduce the scaling variable $(t - t_W)/t_W^\mu$ which was first proposed in the context of polymeric glasses [19]. Fig. 9 shows that the results of the creep experiments measured at different waiting times can be collapsed perfectly on a single master curve. The exponent μ is a function of σ_m ; it varies from 1 at very low stresses (full ageing) to 0 above the yield stress (no ageing). This universal behaviour is one of the characteristic features of ageing. Ageing in glasses is closely related to the existence of a disordered metastable structure which evolves without any characteristic relaxation time. In classical glasses like polymeric glasses, ageing occurs after the glass is brought below its glass transition temperature. In pastes, metastability and ageing appears after flow cessation when the stress is lowered below the yield stress [20]. It has been suggested that ageing in soft dispersions might simply reflect the presence of glass-like dynamics in these materials [21,22]. Recently, ageing has been discovered in other soft dispersions [23].

A microscopic picture of ageing in microgel pastes can be proposed if we come back to the local structure. When pastes are subjected to a large stress, they flow like viscous liquids. When the stress is removed, macroscopic flow stops and the particles get trapped in a metastable arrangement close to that existing in the liquid paste. After flow cessation, the local structure evolves slowly. This occurs because of the contraction, expansion, re-orientation of the facets between microgels under the combined action of thermal fluctuations and of the local stresses. These processes are not purely local. Instead they involve large-scale rearrangements and collective topological changes. Because of this, different spatial configurations with a broad distribution of relaxation times coexist in the paste. At time t_W , those configurations with relaxation times smaller than t_W have relaxed and respond elastically. Subsequently, the response to a stress applied at t_W depends in the waiting time.

4.3. Universality of flow properties

Above the yield stress, pastes flow like viscous liquids. Flow curves are built by applying a stress constant σ and measuring the shear-rate $\dot{\gamma}$ which is reached at steady state. Typical results are shown in Fig. 10 where we have varied the concentration and the solvent viscosity. Similar variations are also obtained when the cross-link density, the ionisation degree, and the ionic strength are varied. All flow curves exhibit the same characteristic shape: a constant stress plateau at low shear-rates followed by a power-law variation at large shear-rates. This behaviour can be found in many other concentrated systems [24]. To get a precise control over the rheology, it is crucial to elucidate the underlying parameters that effectively control the flow properties and the nature of the physical mechanisms at work.

Using the appropriate set of microscopic variables, it is possible to scale all the flow curves onto a universal curve [14]. Our approach is based on the glass-like structure of microgel pastes. When the paste is set into motion, a local distribution of stresses and strains appear in the bulk of the material. If the local strain exceeds the yield strain γ_y , particles escape from their cages and relax to another position. We argue that the duration of a rearrangement is set by the shortest relaxation time. Therefore, it has to be of the order of the relaxation time τ_β . In Fig. 10, we plot the flow curves measured for different experimental pastes as a function of the variable $\dot{\gamma}\tau_\beta$. The stress is scaled by the yield stress. Remarkably, all the flow curves collapse onto a single master curve. The collapse is excellent over many decades. At low-shear rates, the universal flow curve is well approximated by a stress plateau. At high shear-rates, it tends to a power-law with an exponent close to 0.5. This shows that the

competition between structural relaxation and shearing plays a central role in the non-linear paste rheology. At low shear-rates, rearranging particles relax back to local equilibrium before the flow induces a new rearrangement. The flow is quasi-static; the stress remains constant, of the order of the yield stress. At high shear-rates, the shearing motion induces a continuous sequence of rearrangements. Microgels exchange their position very quickly leading to liquid-like behaviour. The stress increases due to viscous dissipation associated with inter-particle friction.

5. Concluding remarks

Suspensions of polyelectrolyte microgels share several features common to other pastes and slurries: elasticity, yielding behaviour, and ageing. The microscopic structure is determined by many experimental parameters such as the cross-link density, the ionisation degree, and the concentration. The macroscopic flow properties exhibit remarkable universality. This enables us to tune the rheological properties at will. In that respect, dispersions of polyelectrolyte microgels appear to be a very nice model system which may help to understand more deeply the properties of colloidal pastes. However, they are also interesting in their own right. Indeed, their capacity to respond strongly to external stimuli makes them ideal in many formulations and applications.

References

- [1] R. Seghrouchni, G. Petekidis, D. Vlassopoulos, G. Fytas, A.N. Semenov, J. Roovers, G. Fleischer, *Europhys. Lett.* 42 (1998) 271.
- [2] J.C. Castaing, C. Allain, P. Auroy, L. Auvray, A. Pouchelon, *Europhys. Lett.* 76 (1996) 153.
- [3] A.P. Gast, *Langmuir* 12 (1996) 4060.
- [4] B.R. Saunders, B. Vincent, *Adv. Colloid Interface Sci.* 80 (1) (1999).
- [5] M.S. Wolfe, *Progr. Org. Coatings* 20 (1992) 487.
- [6] R. Borrega, *Suspensions de microgels polyelectrolytes : propriétés physico-chimiques, rhéologie, écoulement*, Thèse de l'Université Paris VI, 2000.
- [7] M.S. Wolfe, C. Scopazzi, *J. Colloid Interface Sci.* 133 (1989) 265.
- [8] S. Fridrikh, C. Raquois, J.F. Tassin, S. Rezaiguia, *J. Chim. Phys.* 93 (1996) 941.
- [9] See articles in: K. Dusek (Ed.), *Responsive Gels: Volume Transitions I*, Springer-Verlag, Berlin, 1993.
- [10] S. Zhou, B. Chu, *J. Phys. Chem. B* 102 (1998) 1364.
- [11] R. Borrega, M. Cloitre, I. Betremieux, B. Ernst, L. Leibler, *Europhys. Lett.* 47 (1999) 729.
- [12] V.A. Pryamitsin, F.A.M. Leermakers, G.J. Fleer, E.B. Zhulina, *Macromolecules* 29 (1996) 8260; E.Y. Kramarenko, A.R. Khokhlov, K. Yoshikawa, *Macromolecules* 30 (1997) 3383.
- [13] Van Der Werff, C.G. De Kruif, *J. Rheology* 38 (1994) 201.
- [14] M. Cloitre, R. Borrega, F. Monti, L. Leibler, *Phys. Rev. Lett.* 90 (2003), 068303-1.
- [15] L.D. Landau, E.M. Lifshitz, *Theory of Elasticity*, Butterworth-Heinemann, 1995.
- [16] T.G. Mason, J. Bibette, D.A. Weitz, *Phys. Rev. Lett.* 75 (1995) 2051.
- [17] M.D. Lacasse, G.S. Grest, D. Levine, *Phys. Rev. E* 54 (1996) 5436.
- [18] A.D. Gopal, D.J. Durian, *Phys. Rev. Lett.* 75 (1995) 2610.
- [19] L.C.E. Struik, *Physical Aging in Amorphous Polymers and Other Materials*, Elsevier, Amsterdam, 1978.
- [20] M. Cloitre, R. Borrega, L. Leibler, *Phys. Rev. Lett.* 85 (2000) 4820.
- [21] P. Sollich, F. Lequeux, P. Hébraud, M.E. Cates, *Phys. Rev. Lett.* 78 (1997) 2020; P. Sollich, *Phys. Rev. E* 58 (1998) 738.
- [22] S. Fielding, P. Sollich, M.E. Cates, *J. Rheology* 44 (2000) 323.
- [23] L. Cipolletti, S. Manley, R.C. Ball, D.A. Weitz, *Phys. Rev. Lett.* 84 (2000) 2275; C. Derec, A. Ajdari, G. Ducouret, F. Lequeux, *C. R. Acad. Sci.* 1 (IV) (2000) 1115.
- [24] H.A. Barnes, *J. Non-Newton. Fluid Mech.* 81 (1999) 133.